

# The Use of Brushite Calcium Phosphate Cement for Enhancement of Bone-Tendon Integration in an Anterior Cruciate Ligament Reconstruction Rabbit Model

Chun-Yi Wen,<sup>1,2</sup> Ling Qin,<sup>1,2</sup> Kwong-Man Lee,<sup>3</sup> Kai-Ming Chan<sup>1,2</sup>

<sup>1</sup> Department of Orthopaedics and Traumatology, Faculty of Medicine, The Chinese University of Hong Kong, Hong Kong SAR, China

<sup>2</sup> The Hong Kong Jockey Club Sports Medicine and Health Sciences Centre, Faculty of Medicine, The Chinese University of Hong Kong, Hong Kong SAR, China

<sup>3</sup> Lee Hysan Clinical Research Laboratories, The Chinese University of Hong Kong, Hong Kong SAR, China

Received 28 March 2008; revised 16 June 2008; accepted 1 August 2008

Published online 20 October 2008 in Wiley InterScience (www.interscience.wiley.com). DOI: 10.1002/jbm.b.31236

**Abstract:** This study was designed to investigate the osteoconductivity and bioresorption of brushite calcium phosphate cement (CPC) in bone-tendon interface healing after anterior cruciate ligament (ACL) reconstruction. Surgical reconstruction using grafted tendon in bone tunnel was performed bilaterally in 28 skeletal mature rabbits. Brushite CPC was implanted between grafted tendon and bone tunnel of one limb with the contralateral one as the control. A batch of 14 rabbits was sacrificed at 6 and 12 weeks, respectively, after surgery. At each time point, six rabbits were used for micro-CT and subsequent histological examinations, whereas the remaining eight rabbits were used for pull-out testing. The components of brushite CPC-dicalcium phosphate dihydrate matrix degraded rapidly with  $\beta$ -tricalcium phosphate granules left for guiding new bone formation. Brushite CPC augmented the peri-tendon bone volume and promoted bone growth into the healing interface. The ultimate strength and stiffness of the graft-tunnel complexes on experimental side was higher than that of the control by 117% and 102%, respectively, at 6 weeks postoperatively ( $p < 0.05$  for both). The use of brushite CPC caused a paradigm shift in failure mode from intra-tunnel to intra-articular portion at 12 weeks postoperatively ( $p = 0.013$ ). Brushite CPC significantly enhanced the bone-tendon integration after ACL reconstruction, which provided a scientific basis for clinical application.

© 2008 Wiley Periodicals, Inc. *J Biomed Mater Res Part B: Appl Biomater* 89B: 466–474, 2009

**Keywords:** anterior cruciate ligament reconstruction; brushite; calcium phosphate cement; bone-tendon healing; microcomputed tomography

## INTRODUCTION

Anterior cruciate ligament (ACL) rupture is one of the most common knee injuries in sports medicine. Annually, more than 150,000 new ACL rupture cases are recorded in the United States.<sup>1</sup> Surgical reconstruction using tendon grafts in bone tunnel is often performed on patients with ruptured ACL to restore the joint stability.<sup>2</sup> However, the grafted tendon healing to tunneled bone was slower and weaker than bone to bone healing.<sup>3</sup> It was reported that the bone-tendon healing interface remained the weakest link until 3 months after the operation.<sup>4</sup>

Peri-tendon bone healing played an important role in the bone-tendon (B-T) integration.<sup>5–7</sup> The B-T integration is influenced by the peri-tendon bone quantity, which in turn determines the strength of the B-T attachment.<sup>7</sup> It was also found that B-T collagen fibers reconnection was accompanied by progressive bone growth into B-T healing interface.<sup>6</sup> The strength of the B-T attachment correlated with the amount of bone in-growth.<sup>5,6</sup> However, bone tunnel enlargement was common clinically, which indicated peri-tendon bone loss after ACL reconstruction.<sup>8</sup> The tunnel wall may recede from grafted tendon with the gap filled with fibrous tissue, and it was associated with knee laxity.<sup>9</sup>

Hydraulic injectable calcium phosphate (CPC) is a new family of bone substitute, which has been developed as a void filler to augment bone healing.<sup>10</sup> According to the end products of the setting reaction, CPC was further categorized as hydroxyapatite (HA) (HA-CPC) and brushite (dicalcium

Correspondence to: K.-M. Chan (e-mail: kaimingchan@cuhk.edu.hk)

Contract grant sponsor: Research Grant Council Earmarked Grants 06-07, Hong Kong SAR, China; Contract grant number: CUHK4497/06M

© 2008 Wiley Periodicals, Inc.

phosphate dihydrate, DCPD) cements (brushite CPC).<sup>11,12</sup> Various HA-CPC materials, including HA/collagen gel and HA-TCP mixture, have been studied with an attempt to promote B-T integration.<sup>13–15</sup> However, in these previous experimental studies, only decalcified histological technique was used for the evaluation of healing quality. The bioconductivity and bioresorption of CPC in the B-T interface healing has not been clearly explored.<sup>13–15</sup> In addition, the beneficial effect of CPC on the B-T attachment strength was only reported at 1, 2, and 4 weeks postoperatively in previous studies.<sup>14,15</sup> This raised our concerns on whether the slowly degraded HA at the healing interface would be unfavorable for B-T integration in the midterm and long term.

Compared with HA-CPC, the brushite CPC (chronOS™ Inject, RMS Foundation, Bettlach, Switzerland, and Synthes Biomaterials, Switzerland), which was investigated in this study, has exhibited a significantly higher rate of cement resorption and new bone formation without any signs of inflammatory or immunologic response at 2, 4, and 6 months.<sup>16</sup> We hypothesized that brushite CPC filling B-T interface could augment the peri-tendon bone healing and enhance B-T integration at 6 and 12 weeks after ACL reconstruction in a rabbit model. In this study, a nondestructive three-dimensional (3D) microcomputed tomography (micro-CT) was applied to investigate the bioconductivity and bioresorption of the brushite CPC in the peri-tendon bone healing and B-T interface healing in conjunction with non-decalcified histology and pull-out test.

## MATERIALS AND METHODS

### Study Design

Twenty-eight healthy skeletal mature New Zealand white female rabbits (26 weeks old; weight 3.5–4.0 kg) were used for this study. The experiment was approved by the Research Ethics Committee of the authors' institute (Ref No. CUHK06/004/ERG). ACL reconstruction with long digital extensor tendon graft was performed bilaterally on the hind limbs in all rabbits. Brushite CPC was implanted between the grafted tendon and tunneled bone on one limb with the contralateral one as the control. The batch of 14 rabbits was sacrificed at 6 and 12 weeks, respectively, postsurgery. At each time point, six rabbits were used for micro-CT, followed by the fluorescence and light microscopic examinations, whereas the remaining eight rabbits were used for the pull-out test.

### Preparation of the Brushite CPC

The dry component of this cement consisted of 42 wt %  $\beta$ -TCP powder, 31 wt %  $\beta$ -TCP granules, 21 wt % monocalcium phosphate monohydrate, 5 wt % magnesium hydrogen phosphate trihydrate, and a small portion (<1 wt %) of sodium hydrogen pyrophosphate and magnesium sulfate to control the setting time. The liquid component consisted of 0.5% solution of sodium hyaluronate. These two components were mixed together in a custom-made syringe. The

$\beta$ -TCP granules were obtained by the granulation of the  $\beta$ -TCP powder. After setting at body temperature, the cement was biphasic, that is, it consisted of large granules of  $\beta$ -TCP (0.3 mm in diameter), which were embedded in a matrix containing fine DCPD crystals.<sup>17</sup>

### Animal Surgery

ACL reconstruction with long digital extensor tendon graft was performed bilaterally on the hind limbs in all rabbits according to our established protocol.<sup>18</sup> In brief, each rabbit was operated under general anesthesia with 10% ketamine/2% xylazine (Kethalar, 1 mL:1 mL) and maintained sedation with 2.5% sodium phenobarbital injected intravenously (Sigma Chemical, St. Louis, MO). The medial parapatella arthrotomy was done to expose the knee joint. The patella was then dislocated and the infrapatella fat pad was removed to expose the joint cavity. ACL was excised and the transverse meniscal ligament was also removed. The long digital extensor tendon graft of 2.0 mm in diameter was harvested. Graft preparation was done by removing the attached muscle and passing the holding sutures through each end of the tendon graft in an interdigitating whipstitch fashion. The femoral and tibial tunnel was created through the footprint of original ACL using 2.7-mm diameter drill bit. On the experimental side, the cement was injected into the 2.7-mm diameter bone tunnel and shaped on the tunnel wall before passing through the 2.0-mm diameter tendon graft (Figure 1). The graft was then inserted and routed through the bone tunnels via the holding sutures. The graft at the extra-articular exits of the tunnel was fixed with maximum tension to the neighboring soft tissue by secure knots. The wound was closed in layers and wrapped with dressing. The rabbits were allowed for free cage movement after surgery.

### Micro-CT Examination

3D analysis of peri-tendon bone mass and microarchitecture were performed using microCT-40 (Scanco Medical, Brüttisellen, Switzerland) according to our established protocols.<sup>19,20</sup> In brief, the sample was placed with their long axes in the vertical position and immobilized with a foam pad in a cylindrical sample holder, which was filled with 70% ethanol. The femoral and tibial tunnels of each sample were scanned. The continuous scans were prescribed perpendicular to the long axis of the limb at an isotropic resolution of 30  $\mu\text{m}^3$ . The region of interest (ROI) of 3 mm in diameter was defined to cover the bone tunnel region. The same ROI was used in all the samples. The entire tunnel was included for analysis. The acquired 3D data set was first convoluted with a 3D Gaussian filter with a width and support equal to 1.2 and 2, respectively (Figure 2).

It was observed under histological examination that newly formed bone was present in the space left by resorption of DCPD matrix with  $\beta$ -TCP granules left as the guiding structures at 6 weeks onward after surgery. Bone and  $\beta$ -TCP granules were segmented from the marrow and soft

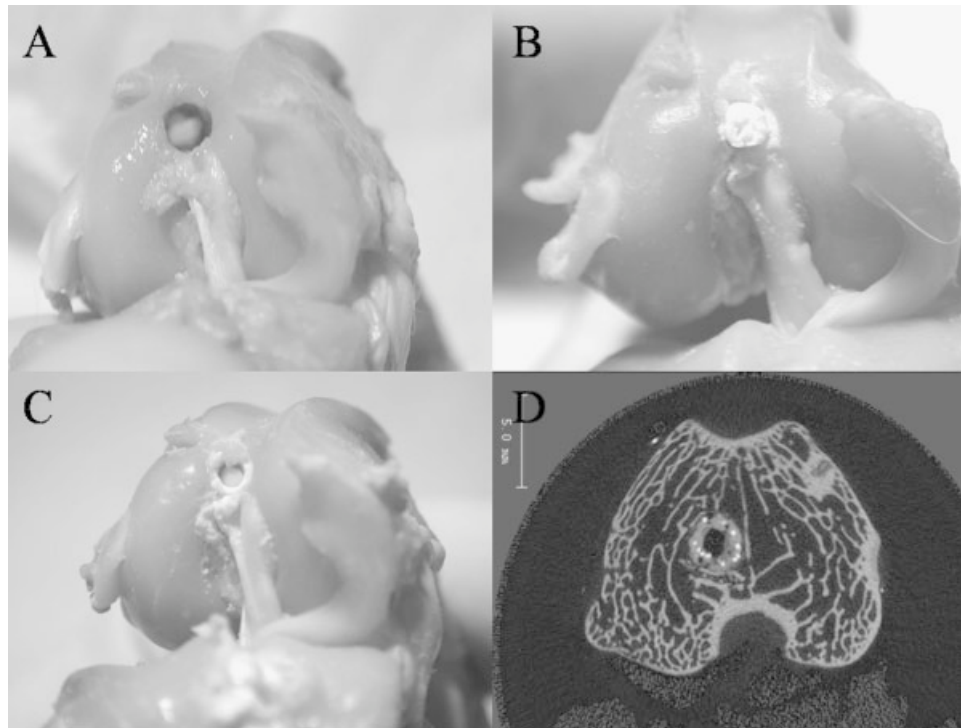


**Figure 1.** Procedures of brushite CPC delivery. (A) Femoral tunnel was drilled; (B) the cement was injected into the bone tunnel; (C) the cement was molded on the tunnel wall before grafted tendon passing through; (D) Micro-CT image showed the cement was evenly distributed around the bone tunnel.

tissue for subsequent analyses using a global thresholding procedure.<sup>21</sup> A threshold equal to or above 350 signified the  $\beta$ -TCP granules; a threshold below 350 and equal to or above 210 represented the bone tissue; a threshold below 210 represented the marrow and soft tissue.

After segmentation, the diameter of  $\beta$ -TCP granules was calculated by the parameter “trabeculae thickness.” The peri-tendon bone volume and architecture was calculated using the built-in analysis program of the micro-CT,

including the fraction of bone volume/tissue volume (BV/TV), connectivity density (Conn.D), structure model index (SMI), trabecular number (Tb.N), trabecular thickness (Tb.Th), and trabecular spacing (Tb.Sp).

#### Fluorescence Microscopical Examination

Newly formed bone was labeled sequentially with fluorescent dyes *in vivo*. The fluorescent dyes, namely xylenol orange

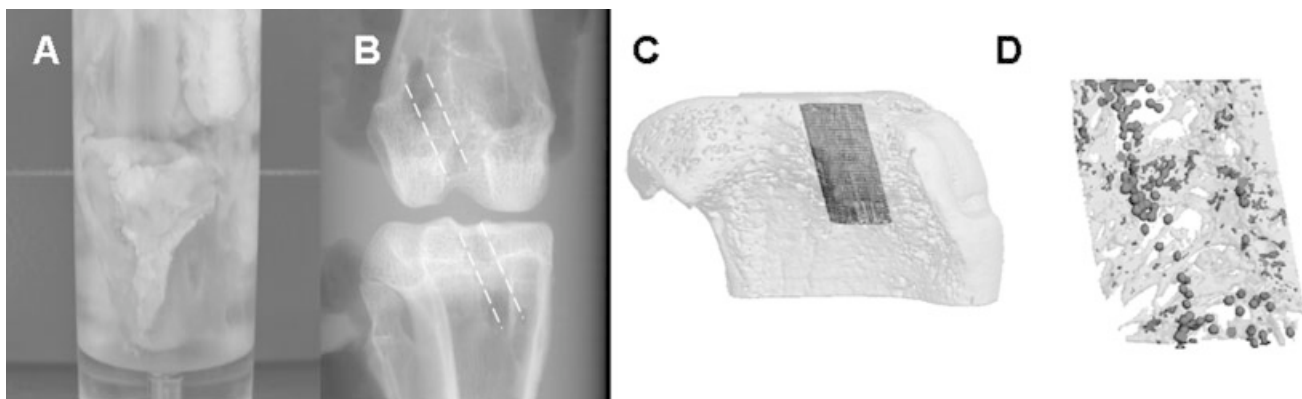


**Figure 2.** Procedures of micro-CT scan and analysis. (A) The samples were placed with its long axes in the vertical position in a cylindrical sample holder; (B) the femoral and tibial tunnel (dot line) were scanned perpendicular to the long axis of limb; (C) for an instance, the region of interest of 3 mm in diameter covering entire tunnel region was harvested from tibial tunnel for analysis; (D) the  $\beta$ -TCP granules and bone tissue were segmented from bone marrow and soft tissue by thresholding procedures for subsequent analysis.

(90 mg/kg body weight) and calcein green (10 mg/kg body weight, both from Sigma-Aldrich GmbH, USA), were injected subcutaneously and sequentially into the rabbits of 6-week group at week 3 and 4, and of 12-week group at week 9 and 10 postoperatively. After euthanasia, the samples were dehydrated sequentially in ethanol and xylene and infiltrated with methylmethacrylate (MMA). The embedded specimens were sectioned perpendicularly to the bone tunnels by saw microtome (SP 1600, Leica, Germany). The sections in the middle portion of the bone tunnel were grinded and polished to 80–100  $\mu\text{m}$  for the fluorescence microscopic examination by grinder/polisher (RotoPol-21, Struers, Denmark). The sections were visualized fluorometrically under ultra-violet light as our established protocol.<sup>22</sup>

### Histology

The MMA-resined sections were stained with metachromatic toluidine blue. Cells and matrix at the healing interface were examined under microscopic imaging system (Leica Q500MC, Leica Cambridge, Cambridge, UK). The collagen fibers connection from bone to tendon was examined under the polarized microscopy (Leica Q500MC, Leica Cambridge).<sup>22</sup>

### Biomechanical Testing

The graft-tunnel complexes were harvested and stored at  $-20^{\circ}\text{C}$  until biomechanical testing within 1 month after the surgery. After the samples were thawed at room temperature, the knee joints were carefully dissected to remove the surrounding soft tissue until only ACL graft was left as the physical connection between femur and tibia. The fixations by suture on both sides were removed when testing. The graft-tunnel complexes were fixed with custom-made clamps, allowing a tensile loading along the long axis of the graft in a material testing machine (H25K-S, Hounsfield Test Equipment, Surrey, UK). A preload of 1 N and a load displacement rate of 50 mm/min tensile force were applied to the graft-tunnel complex until failure. The failure mode was recorded and the load to failure (N) and stiffness (N/mm) were calculated based on the load displacement curve.

### Statistical Methods

The experimental and the control sides were compared in respect of the volume and architecture of bone growth into the tunnel, the bone formation rate, the ultimate strength, and the stiffness of the graft-tunnel complexes using Wilcoxon Signed Rank test. The failure modes between two sides were also compared using Fisher's exact test. The level of significance was set at  $p < 0.05$ . All the data analysis was performed using SPSS 15.0 analysis software (SPSS, Chicago, IL).

## RESULTS

### Micro-CT Analysis

As shown in Table I and Figure 3, the fraction of BV/TV in vicinity of the grafted tendon on the experimental side

TABLE I. Comparison of Peri-Graft Bone Volume and Architecture Between Experimental Side and Control

Parameters (Mean $\pm$ SD)	6 Weeks				12 Weeks			
	Experimental Side		Control Side		Experimental Side		Control Side	
	Femur	Tibia	Femur	Tibia	Femur	Tibia	Femur	Tibia
BV/TV (0–1)	0.064 $\pm$ 0.039	0.084 $\pm$ 0.047*	0.068 $\pm$ 0.033	0.045 $\pm$ 0.027	0.144 $\pm$ 0.064*	0.087 $\pm$ 0.039*	0.064 $\pm$ 0.034	0.060 $\pm$ 0.028
Con. D. (1/mm <sup>3</sup> )	1.26 $\pm$ 1.51	3.04 $\pm$ 2.14*	1.39 $\pm$ 0.75	0.69 $\pm$ 0.58	3.52 $\pm$ 2.85*	2.22 $\pm$ 1.19*	0.83 $\pm$ 0.55	0.60 $\pm$ 0.33
SMI (0–3)	1.20 $\pm$ 0.95*	0.71 $\pm$ 0.45*	2.47 $\pm$ 0.72	2.70 $\pm$ 0.67	1.27 $\pm$ 0.83*	1.40 $\pm$ 0.65*	2.34 $\pm$ 0.67	2.40 $\pm$ 0.64
Tb.N (1/mm)	0.98 $\pm$ 0.24*	0.70 $\pm$ 0.19*	0.76 $\pm$ 0.49	0.50 $\pm$ 0.11	1.24 $\pm$ 0.68*	0.69 $\pm$ 0.09*	0.65 $\pm$ 0.24	0.55 $\pm$ 0.09
Tb.Th (mm)	0.11 $\pm$ 0.02	0.13 $\pm$ 0.03	0.16 $\pm$ 0.01	0.16 $\pm$ 0.03	0.16 $\pm$ 0.03	0.15 $\pm$ 0.03	0.17 $\pm$ 0.03	0.19 $\pm$ 0.04
Tb.Sp (mm)	1.16 $\pm$ 0.26*	1.60 $\pm$ 0.29*	1.67 $\pm$ 0.69	2.15 $\pm$ 0.50	1.09 $\pm$ 0.65*	1.54 $\pm$ 0.16*	1.77 $\pm$ 0.60	1.95 $\pm$ 0.34

Note: \*\* $p < 0.05$ .

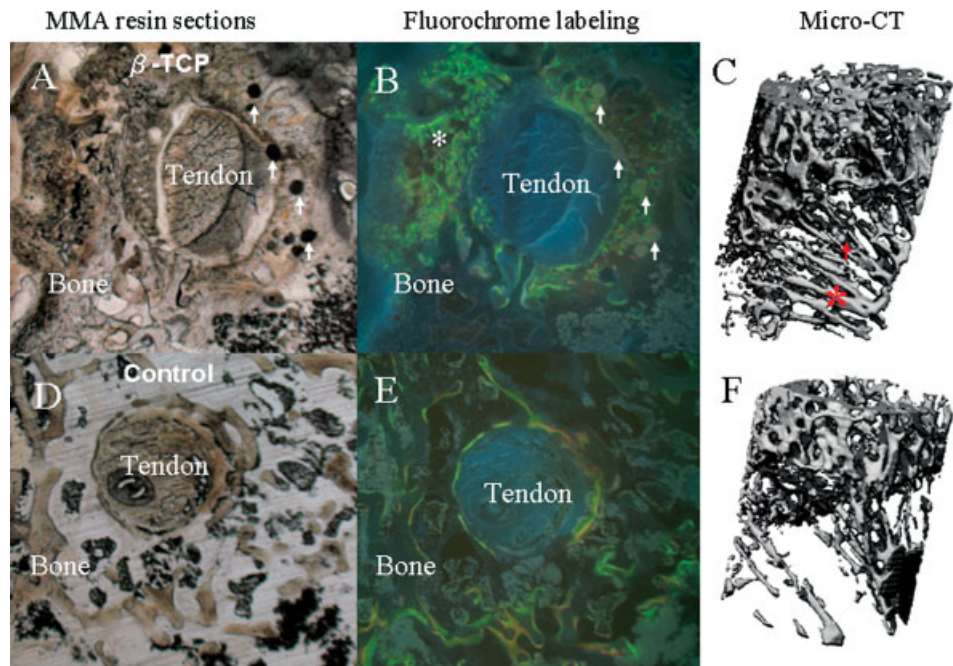


**Figure 3.** The representative images showing bone growth into the tunnel during bonetendon healing on both  $\beta$ -TCP-treated side (A–C) and control side (D–F) at 6 weeks postoperatively. (A and B) massive new bone formation (star) was observed on the experimental side with  $\beta$ -TCP granules (arrow) embedded bone tunnel wall. (D and E) On the control side, new bone formation was found in vicinity of grafted tendon. (C and F) Results of micro-CT 3D reconstruction revealed that there was more new bone formation (star) on experimental side than the control;  $\beta$ -TCP granules (arrow) were noted inside trabeculae (original magnification of A, B, C, and D:  $\times 16$ ). [Color figure can be viewed in the online issue, which is available at [www.interscience.wiley.com](http://www.interscience.wiley.com).]

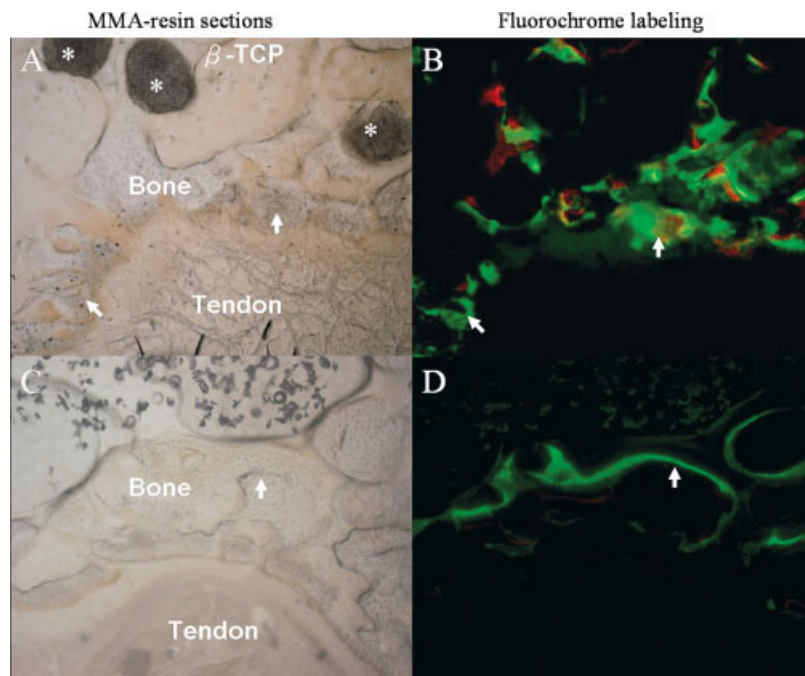


**Figure 4.** The representative microphotographs showing the location and direction of bone in-growth at healing interface on experimental side (A, B) and control side (C, D) at week 6 after surgery. (A and B) On the experimental side, the boundary between bone and tendon became obscure with massive bone growth into the interface (arrow);  $\beta$ -TCP granules (star) were embedded in newly formed bone. (C and D) On the control side, the fibrous interface was distinct between tendon and bone; newly formed bone was observed inside bone tunnel wall instead of at B-T healing interface (arrow) (original magnification:  $\times 100$ ). [Color figure can be viewed in the online issue, which is available at [www.interscience.wiley.com](http://www.interscience.wiley.com).]

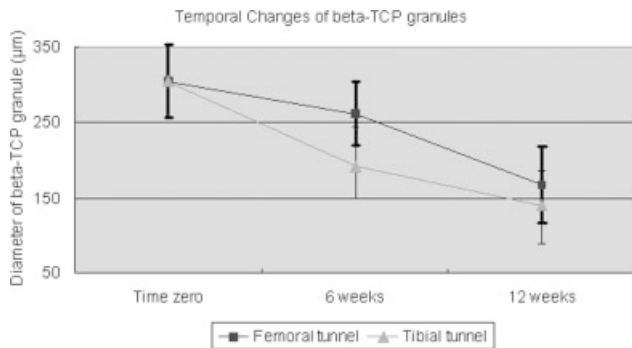


**Figure 5.** The graph showing the temporal changes of  $\beta$ -TCP granules.

was significantly higher than the control at both 6 weeks and 12 weeks postoperatively ( $p < 0.001$  for both). The peri-tendon bone microarchitecture on the experimental side was also superior to the control, which showed more trabeculae number, less trabeculae space, and higher connectivity. After treatment, the peri-tendon bone consisted of more plate-like trabeculae than the rod-like trabeculae, which was indicated by the SMI showing the maturity of bone microarchitecture.

Interestingly at 6 weeks postoperatively, the fraction of BV/TV in femoral tunnel was higher than that in tibial tunnel on the control side; whereas on the experimental side, the BV/TV in tibial tunnel was significantly higher than that of the femoral tunnel ( $p < 0.05$ ).

As shown in Figure 5, the diameter of  $\beta$ -TCP granules decreased with time postoperatively ( $p < 0.05$ ). It was noted that the resorption rate of  $\beta$ -TCP granules was faster in the tibial tunnel than the femoral tunnel at 6 weeks after surgery ( $p < 0.05$ ).

#### Fluorescence Microscopic Examination

As shown in Figures 3 and 4, it was observed that there was massive new bone formation in the vicinity of the grafted tendon on the experimental side at 6 weeks postoperatively, where newly formed bone progressively grew into B-T healing interface. In contrast, newly formed bone was observed on the bone tunnel wall around the grafted tendon but the fluorescence signals were not observed at the bone front of the B-T healing interface. There was no significant difference in the rate of new bone formation between the experimental and the control sides at 6 weeks after surgery ( $17 \pm 5 \mu\text{m}/\text{week}$  on the control side and  $19 \pm 7 \mu\text{m}/\text{week}$  on the experimental side,  $p = 0.317$ ). At 12 weeks after surgery, there was also no significant difference in the rate of new bone formation on both sides ( $p = 0.154$ ).

#### Light Microscopic Examination

At 6 weeks postoperatively, the fibrous interface was distinct between the tendon and bone with a few collagen fibers on the control side. The osteoblasts (lining cells)

were observed at the bone front in the B-T healing interface. In contrast, the B-T interface became obscure on the experimental side and the  $\beta$ -TCP granules were embedded in the newly formed bone (Figures 3 and 5). The densely stained newly formed bone was found at the bone front at the B-T healing interface; the chondrocyte-like cells were observed at the healing interface with organized collagen fibers reconnection from the bone to tendon (Figure 6).

At week 12 postoperatively, the fibrous interface narrowed with smooth and distinct boundary between the bone and tendon on the control side. On the experimental side, the grafted tendon directly connected with the tunneled bone with the diminished B-T interface; no chondrocyte-like cells were observed. The remnant of  $\beta$ -TCP granules were embedded inside the mature bone tunnel wall.

#### Biomechanical Testing Results

As shown in Table II, the ultimate strength and stiffness of the graft-tunnel complexes on the experimental side was significantly better than that of the control by 117% and 102%, respectively, at 6 weeks postoperatively ( $p < 0.05$  for both). The use of brushite CPC caused a paradigm shift in the failure modes of the graft-tunnel complexes from the tibial tunnel to the femoral tunnel ( $p = 0.035$ ).

At 12 weeks after surgery, the ultimate strength and stiffness of the graft-tunnel complexes on the experimental side was significantly better than that of the control by 55% and 34%, respectively ( $p < 0.05$  for both). The use of brushite CPC caused a paradigm shift in the failure modes of the graft-tunnel complexes from the intra-tunnel to the intra-articular portion ( $p = 0.013$ ).

#### DISCUSSION

This experimental study systemically investigated the osteoconductivity and bioresorption of brushite CPC in B-T healing after ACL reconstruction. DCPD matrix dissolved and decreased in amount in a short term *in vivo*.<sup>16,17,23</sup> At the time points set for observations in this study, the newly formed bone was present in the space left by the resorption of the DCPD matrix, with  $\beta$ -TCP granules acting as guiding structures. The  $\beta$ -TCP granules provided a large osteoconductive surface for new bone formation without affecting the rate of bone formation. The use of brushite CPC promoted progressive bone growth into the B-T healing interface and direct collagen fibers reconnection between the tunneled bone and the grafted tendon. It may account for the improvement of the B-T attachment strength after treatment. These findings supported our hypothesis that the use of brushite CPC could enhance B-T integration after ACL reconstruction. It was considered that brushite CPC might be superior to HA-CPC with regard to its long-term beneficial effect and fast resorption, yet direct comparative studies would be relevant to confirm our hypothesis.

Actually, various methods such as biological modalities, including growth factors and mesenchymal stem cells, have been extensively explored in an attempt to enhance the B-T

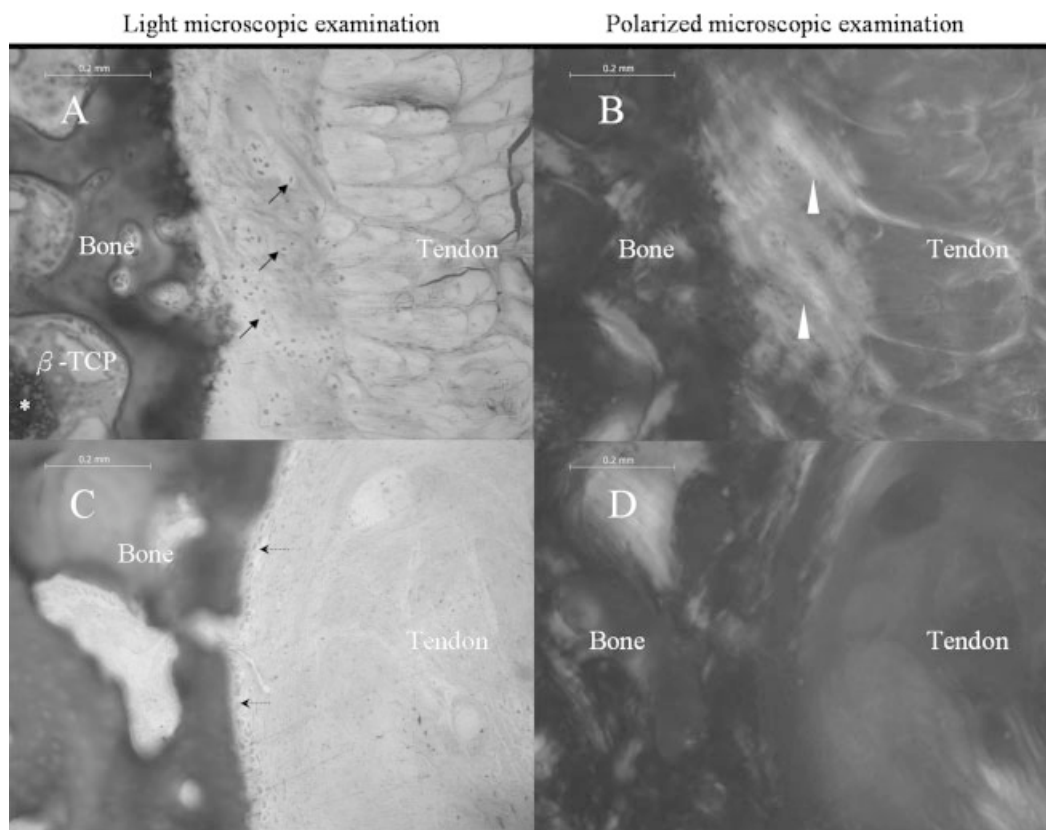


**Figure 6.** The representative microphotographs showing the bone-tendon healing interface tissue on experimental side (A, B) and the control (C, D) at week 6 after surgery. (A and B) Chondrocyte-like cells (arrow) and densely stained new bone formation were observed at B-T healing interface on the experimental side ( $\beta$ -TCP granule labeled by star); organized collagen fibers in bundle (triangle) reconnected bone to tendon. (C and D) On the control side, fibrous interface tissue was observed with osteoblasts lining (arrow with dot line) along the bone front; no direct B-T collagen fiber connection was observed (original magnification:  $\times 200$ ).

integration.<sup>24–29</sup> The use of CPC had its uniqueness to provide initial graft fixation immediately after operation as well as its bioconductivity in comparison with the aforementioned methods.<sup>30,31</sup> However, the tendon-cement interface remained the weakest site.<sup>30</sup> In this study, we demonstrated that the use of brushite CPC caused a paradigm shift in the failure mode of graft-tunnel complexes with healing over time, from intra-tunnel healing interface to intra-articular tendinous portion.

The use of brushite CPC was helpful to provide a large and stable bone bed for the grafted tendon anchorage. As shown by micro-CT evaluation, the use of brushite CPC not only increased peri-tendon bone volume and the number of trabeculae, but also improved its connectivity and maturity. The presence of  $\beta$ -TCP granules in injectable bone cement may help to maintain the transient biomechanical function of the implanted bone and to promote the formation of good-quality new bone.<sup>32</sup>

**TABLE II. Biomechanical Data and Sites of Failure**

Group	Mean $\pm$ SD		Site of Failure (Number of Samples)		
	Load to Failure (N)	Stiffness (N/mm)	Femoral Tunnel	Intra-Articular Midsubstance	Tibial Tunnel
6 weeks					
Treated side ( $n = 8$ )	94 $\pm$ 42	31 $\pm$ 11	5	2	1
Control side ( $n = 8$ )	43 $\pm$ 11	15 $\pm$ 4	1	0	7
12 weeks					
Treated side ( $n = 8$ )	60 $\pm$ 25	22 $\pm$ 6	1	5	2
Control side ( $n = 8$ )	39 $\pm$ 14	16 $\pm$ 8	0	0	8

It was observed under histological examination that the chondrocyte-like cells clustered at the B-T healing interface on the experimental side, whereas the distinct fibrous tissue was present between bone and tendon on the control side. Mutsuzaki et al.<sup>33</sup> also reported similar findings. They soaked the grafted tendon in solution to yield calcium phosphate crystal deposition with the end-product DCPD on the tendon surface before implantation. They reported regeneration of fibrocartilage between tendon and bone at 4 weeks postoperatively on the experimental side. Thus, the presence of cartilaginous interface on the experimental side might be associated with DCPD matrix—the component of brushite CPC in this study. The underlying mechanism of the brushite CPC on chondrogenesis in the B-T healing needs to be further investigated. For the long term, such cartilaginous tissue was replaced with the progressive bone in-growth, which resembled endochondral ossification. It was known that the development of ligament-bone attachment underwent endochondral ossification.<sup>34</sup> We considered that the use of brushite CPC might be helpful for the reestablishment of a native ligament-bone attachment.

Local biological environment was different in the trabecule-rich femoral tunnel from the marrow-rich tibial tunnel. According to the results of the previous experimental study, B-T healing was better in a trabecule-rich femoral tunnel histologically.<sup>7</sup> The similar results were also observed in our study, that is, the peri-tendon bone volume in tibial tunnel was significantly lower than that in femoral tunnel. Grafted tendon was prone to be pulled out of the tibial tunnel in the natural healing process, which indicated that the B-T attachment strength was lower on the tibial side. The peri-tendon bone volume in the marrow-rich tibial tunnel significantly increased after treatment, which exceeded that in the femoral tunnel. This might be a cause of the failure sites of the graft-tunnel complexes on the experimental side shifted from the tibial tunnel to the femoral tunnel at 6 weeks postoperatively. This study also showed that the grafted tendon was prone to be pulled out of the bone tunnel with a lower fraction of BV/TV in the vicinity of the grafted tendon. This finding also suggested that nondestructive 3D micro-CT was a novel approach for an objective evaluation of the quality of B-T healing in bone tunnel.

The bioresorption rate of  $\beta$ -TCP granules varied in the femoral and the tibial tunnel. This finding was consistent with the previous study, which showed that the type and extent of the cement degradation depended on the implantation sites.<sup>35</sup> It was known that the faster resorbed CPC were degraded by macrophages and the giant cells, whereas the slower resorbed CPC (months–years) were decomposed by the osteoclast-type cells in the trabecular bone.<sup>36</sup> In intra-articular tunnel healing, macrophages in synovial fluid were prone to be tracked in the tibial tunnel after ACL surgery.<sup>8</sup> It was postulated that the disparity of local biological milieu in the femoral and the tibial tunnel might explain the site-specific response of  $\beta$ -TCP granules.

## CONCLUSION

In this study, we demonstrated that brushite CPC filling the B-T healing interface resulted in rapid bone-tendon integration in the mid- and long-term after ACL reconstruction in a rabbit model. Our experimental finding might open up a new area for the use of brushite CPC and provide a basis for its potential clinical validation and application to enhance the B-T healing interface integration after ACL reconstruction.

The authors thank Margaret Wan-Nar Wong, Po-Yee Lui, and Sai-Chuen Fu who provided expertise at academic meetings, as well as Hui-Yan Yeung, Chun-Wai Chan, Grace Ho, and Anita Wai-Ting Shum who provided the technical assistance.

## REFERENCES

1. Miyasake KC, Daniel D, Stone ML, Hirshman P. The incidence of knee ligament injuries in the general population. *Am J Knee Surg* 1991;4:3–8.
2. Woo SL, Wu C, Dede O, Vercillo F, Noorani S. Biomechanics and anterior cruciate ligament reconstruction. *J Orthop Surg* 2006;1:2.
3. Tomita F, Yasuda K, Mikami S, Sakai T, Yamazaki S, Tohyama H. Comparisons of intraosseous graft healing between the doubled flexor tendon graft and the bone-patellar tendon-bone graft in anterior cruciate ligament reconstruction. *Arthroscopy* 2001;17:461–476.
4. Goradia VK, Rochat MC, Grana WA, Rohrer MD, Prasad HS. Tendon-to-bone healing of a semitendinosus tendon autograft used for ACL reconstruction in a sheep model. *Am J Knee Surg* 2000;13:143–151.
5. Ma CB, Kawamura S, Deng XH, Ying L, Schneidkraut J, Hays P, Rodeo SA. Bone morphogenetic proteins-signaling plays a role in tendon-to-bone healing: A study of rhBMP-2 and noggin. *Am J Sports Med* 2007;35:597–604.
6. Rodeo SA, Armoczkay SP, Torzilli PA, Hidaka C, Warren RF. Tendon-healing in a bone tunnel. A biomechanical and histological study in the dog. *J Bone Joint Surg Am* 1993;75:1795–1803.
7. Grassman SR, McDonald DB, Thornton GM, Shrive NG, Frank CB. Early healing processes of free tendon grafts within bone tunnels is bone-specific: A morphological study in a rabbit model. *Knee* 2002;9:21–26.
8. Wilson TC, Kantaras A, Atay A, Johnson DL. Tunnel enlargement after anterior cruciate ligament surgery. *Am J Sports Med* 2004;32:543–549.
9. Webster KE, Chiu JJ, Feller JA. Impact of measurement error in the analysis of bone tunnel enlargement after anterior cruciate ligament reconstruction. *Am J Sports Med* 2005;33:1680–1687.
10. LeGeros RZ. Properties of osteoconductive biomaterials: Calcium phosphates. *Clin Orthop Relat Res* 2002;395:81–98.
11. Lu J, Descamps M, Dejoui J, Koubi G, Hardouin P, Lemaitre J, Proust JP. The biodegradation mechanism of calcium phosphate biomaterials in bone. *J Biomed Mater Res* 2002;63:408–412.
12. Bohner M. Calcium orthophosphates in medicine: From ceramics to calcium phosphate cements. *Injury* 2000;31 (Suppl 4):37–47.
13. Ishikawa H, Koshino T, Takeuchi R, Saito T. Effects of collagen gel mixed with hydroxyapatite powder on interface between newly formed bone and grafted achilles tendon in rabbit femoral bone tunnel. *Biomaterials* 2001;22:1689–1694.

14. Huangfu X, Zhao J. Tendon-bone healing enhancement using injectable tricalcium phosphate in a dog anterior cruciate ligament reconstruction model. *Arthroscopy* 2007;23:455–462.
15. Tien YC, Chih TT, Lin JH, Ju CP, Lin SD. Augmentation of tendon-bone healing by the use of calcium-phosphate cement. *J Bone Joint Surg Br* 2004;86:1072–1076.
16. Apelt D, Theiss F, El-Warrak AO, Zlinszky K, Bettschart-Wolfisberger R, Bohner M, Matter S, Auer JA, von Rechenberg B. In vivo behavior of three different injectable hydraulic calcium phosphate cements. *Biomaterials* 2004;25:1439–1451.
17. Theiss F, Apelt D, Brand B, Kutter A, Zlinszky K, Bohner M, Matter S, Frei C, Auer JA, von Rechenberg B. Biocompatibility and resorption of a brushite calcium phosphate cement. *Biomaterials* 2005;26:4383–4394.
18. Wen C, Lui P, Wong MW-N, Fu S, Lee K, Qin L, Chan K. Local bone loss after anterior cruciate ligament reconstruction—A peripheral quantitative computed tomographic study in a rabbit model. *Hong Kong J Orthop Surg* 2006;10 (Suppl):24.
19. Siu WS, Qin L, Cheung WH, Leung KS. A study of trabecular bones in ovariectomized goats with micro-computed tomography and peripheral quantitative computed tomography. *Bone* 2004;35:21–26.
20. Yingjie H, Ge Z, Yisheng W, Ling Q, Hung WY, Kwoksui L, Fuxing P. Changes of microstructure and mineralized tissue in the middle and late phase of osteoporotic fracture healing in rats. *Bone* 2007;41:631–638.
21. Jones AC, Arns CH, Sheppard AP, Huttmacher DW, Milthorpe BK, Knackstedt MA. Assessment of bone ingrowth into porous biomaterials using micro-CT. *Biomaterials* 2007;28: 2491–2504.
22. Lu H, Qin L, Fok P, Cheung W, Lee K, Guo X, Wong W, Leung K. Low-intensity pulsed ultrasound accelerates bone-tendon junction healing: A partial patellectomy model in rabbits. *Am J Sports Med* 2006;34:1287–1296.
23. Bohner M, Theiss F, Apelt D, Hirsiger W, Houriet R, Rizzoli G, Gnos E, Frei C, Auer JA, von Rechenberg B. Compositional changes of a dicalcium phosphate dihydrate cement after implantation in sheep. *Biomaterials* 2003;24:3463–3474.
24. Anderson K, Seneviratne AM, Izawa K, Atkinson BL, Potter HG, Rodeo SA. Augmentation of tendon healing in an intra-articular bone tunnel with use of a bone growth factor. *Am J Sports Med* 2001;29:689–698.
25. Martinek V, Latterman C, Usas A, Abramowitch S, Woo SL, Fu FH, Huard J. Enhancement of tendon-bone integration of anterior cruciate ligament grafts with bone morphogenetic protein-2 gene transfer: A histological and biomechanical study. *J Bone Joint Surg Am A* 2002;84:1123–1131.
26. Chen CH, Liu HW, Tsai CL, Yu CM, Lin IH, Hsiue GH. Photoencapsulation of bone morphogenetic protein-2 and periosteal progenitor cells improve tendon graft healing in a bone tunnel. *Am J Sports Med* 2008;36:461–473.
27. Lim JK, Hui J, Li L, Thambyah A, Goh J, Lee EH. Enhancement of tendon graft osteointegration using mesenchymal stem cells in a rabbit model of anterior cruciate ligament reconstruction. *Arthroscopy* 2004;20:899–910.
28. Sasaki K, Kuroda R, Ishida K, Kubo S, Matsumoto T, Mifune Y, Kinoshita K, Tei K, Akisue T, Tabata Y, Kurosaka M. Enhancement of tendon-bone osteointegration of anterior cruciate ligament graft using granulocyte colony-stimulating factor. *Am J Sports Med* 2008;36:1519–1527.
29. Ju YJ, Muneta T, Yoshimura H, Koga H, Sekiya I. Synovial mesenchymal stem cells accelerate early remodeling of tendon-bone healing. *Cell Tissue Res* 2008;332:469–478.
30. Robertson WJ, Hatch JD, Rodeo SA. Evaluation of tendon graft fixation using alpha-BSM calcium phosphate cement. *Arthroscopy* 2007;23:1087–1092.
31. Mayr HO, Hube R, Bernstein A, Seibt AB, Hein W, von Eisenhart-Rothe R. Beta-tricalcium phosphate plugs for press-fit fixation in ACL reconstruction—A mechanical analysis in bovine bone. *Knee* 2007;14:239–244.
32. Flautre B, Maynou C, Lemaitre J, Van Landuyt P, Hardouin P. Bone colonization of beta-TCP granules incorporated in brushite cements. *J Biomed Mater Res* 2002;63: 413–417.
33. Mutsuzaki H, Sakane M, Nakajima H, Ito A, Hattori S, Miyana Y, Ochiai N, Tanaka J. Calcium-phosphate-hybridized tendon directly promotes regeneration of tendon-bone insertion. *J Biomed Mater Res A* 2004;70:319–327.
34. Gao J, Messner K, Ralphs JR, Benjamin M. An immunohistochemical study of entheses development in the medial collateral ligament of the rat knee joint. *Anat Embryol (Berl)* 1996;194:399–406.
35. Constantz BR, Barr BM, Ison IC, Fulmer MT, Baker J, McKinney L, Goodman SB, Gunasekaran S, Delaney DC, Ross J, Poser RD. Histological, chemical, and crystallographic analysis of four calcium phosphate cements in different rabbit osseous sites. *J Biomed Mater Res* 1998;43:451–461.
36. Ooms EM, Wolke JG, van der Waerden JP, Jansen JA. Trabecular bone response to injectable calcium phosphate (Ca-P) cement. *J Biomed Mater Res* 2002;61:9–18.